Journal of Materials and Environmental Science
ISSN : 2028-2508
e-ISSN : 2737-890X
CODEN : JMESCN

J. Mater. Environ. Sci., 2026, Volume 17, Issue 5, Page 752-764

http://www.jmaterenvironsci.com

Spatial mapping of soil salinity using different interpolation techniques: a case study from the region of Mahdia (Eastern Tunisia)

Louati D. [1]*, Majdoub R. [2], Rigane H. [3], Abida H. [1]

[1]*Laboratory GEOMODELE, Faculty of Sciences, University of Sfax, Soukra Road Km 4, BP 1171, 3000, Sfax, Tunisia*
[2]*Laboratory of Research in Management and Control of Animal and Environmental Resources in Semi-Arid Ecosystem (LR18AGR01), Higher Agronomic Institute of Chott Meriem, University of Sousse, BP 42, 4042 Chott Mariem, Sousse, Tunisia*
[3]*Laboratory of Environmental Sciences and Sustainable Development (LR18ES32), University of Sfax, IPEIS, BP172, Soukra Road Km 4, BP 1171, 3000, Sfax, Tunisia*

**Corresponding author, Email address: dhouhaloua7@gmail.com*

Received *07 Dec 2025,*
Revised *05 May 2026,*
Accepted *10 May 2026*

Keywords:
- ✓ *Interpolation;*
- ✓ *Inverse Distance Weighted Method;*
- ✓ *Ordinary Kriging;*
- ✓ *Salinity;*
- ✓ *Semi-variogram*

Citation*: Louati D., Majdoub D., Rigane H. Abida H. (2026) Spatial mapping of soil salinity using different interpolation techniques: a case study from the region of Mahdia (Eastern Tunisia), J. Mater. Environ. Sci., 17(5), 752-764.*

Abstract: This study aims to model soil salinity spatial distribution using ordinary kriging and Inverse Distance Weighted interpolation methods. Soil samples were collected from the irrigated perimeter of Zelba of the region of Mahdia (Eastern Tunisia). Electrical conductivity ($EC_{1/5}$) measurement were interpolated with the Gaussian semi-variogram model using ordinary kriging. Variogram parameters showed that the nugget effect values are relatively low ($C_0 \leq 10^{-4}$). The nugget effect/sill ratio is less than 25%, the correlation coefficient (r^2) is close to 1 and the range values varied between 607 and 1520 m. Cross validation was adopted to validate the semi-variogram. Results showed that the correlation coefficient values are close to 1 and the regression coefficient (R) values ranged between 0.85 and 0.99 indicating that $EC_{1/5}$ spatial autocorrelation between sampled values is strongly positive. Obtained soil salinity maps using two interpolation methods showed similar distribution patterns. The southern and the southwestern parts of the perimeter are the most affected by salinity, especially in depth. The low salinity recorded in the northern section of the area may be linked to its closeness to the water well. This area receives a greater water supply, due to overflow from the nearby basins, which enhances the salts leaching in depth.

1. Introduction

Soil is a fundamental component of our planet and plays an important role in promoting sustainable development (Caglar and Dengiz, 2025). It is a crucial life supporter and nutriment provider (Gama, 2023). However, soil salinization is a significant global issue that affects soil functions, especially in arid and semi-arid regions, where evaporation outweigh precipitation. As reported by (Bartels *et al.*, 2005; Shrivastava *et al.*, 2015; Fu *et al.*, 2021; Chetouani *et al.*, 2023; Laita *et al.*, 2024a) soil salinization is one of the most critical environmental problems and a serious land degradation factor limiting productivity worldwide. According to (Shrivastava *et al.*, 2015), (Bartels *et al.*, 2005), (Fu *et al.*, (2021) more than $8{\times}10^8$ hm^2 of land worldwide is affected by salinization, accounting for more than 6% of the total. As reported by (Setia *et al.*, 2013) soil salinization affects about 3.1% (397 million hectares) of the total global land area. Moreover, soil salinization is expected to increase to an alarming rate exceeding 50% by 2025 (Jamil *et al*., 2011). Indeed, there are two forms of salinization. Primary salinization originates from parent material weathering and secondary salinization is induced by human activities (Uri, 2018).

Irrigation with saline water is considered a form of secondary salinization. As reported by (Haj Amor *et al*., 2022) frequent irrigation using saline water can accelerate the soil salinization process, seriously degrading the agricultural soil quality in different ways. Besides, a high concentration of soluble salts in the soil, can cause physico-chemical deterioration of the soil which leads to the dispersion of the clay particles and structural damage (Awedat *et al*., 2021; Laita *et al*., 2024b). Soluble salts accumulation in soil profile can also reduce soil fertility making then a difficulty for crops to grow (Yu *et al*., 2014). Electrical conductivity (EC) of soil irrigated with saline water reflects the actual situation of the soil salinity (Yang *et al*., 2016). According to (Wang *et al*., 2024) higher values of (EC) indicate a risk of soil salinization. The measurements of (EC) can be converted to soil salinity values by linear equations, then soil salinization can be obtained (Wang *et al*., 2022). Thus, understanding the spatial soil salinity variation behavior is crucial for natural resources management to maintain sustainability.

Spatial mapping of soil salinity has considerably improved our understanding of soil salinization processes. It provides valuable information for land reclamation and restoration in making effective site-specific management decisions. According to (Hassani *et al*., 2021) digital mapping of EC is essential in order to comprehend changes about soil salinization. Many interpolation methods have been used for the spatial predictions and mapping of soil salinity including geostatistical methods like ordinary kriging (OK) and the method of Inverse Distance Weighted method (IDW). Ordinary kriging (OK) is a geostatistical method that is widely used for spatial interpolation. It was applied by (Panday *et al*., 2018), to determine soil chemical distribution over agricultural lands of the Bara district (Nepal). It was also used by (Sahbeni and Székely, 2021) to map salinity spatial distribution in the great Hungarian Plain and to compare the predictive performance of four kriging methods including ordinary kriging. (Abdennour *et al*., 2019) used ordinary kriging for salinity levels analysis in the irrigated perimeter of EL Ghrous in south-eastern Algeria. The 'Spatial analyst' tool is an add-on module for ArcView GIS 3.2 software for performing powerful spatial modeling and complex analysis. This module was used to create a continuous salinity map from sampling points. It was applied by many researchers, including (Gribb *et al*., 2005) who applied the ArcView 'spatial analyst' in order to determine the potential habitat for seven endangered, threatened or candidate species in Albany County, Wyoming, USA. IDW interpolation method is a mathematical technique which assumes a closer value and shows more similarity than the further value with its characteristics (Tomaszewski, 2021). As reported by (Abdelrrahman *et al*., 2021) the IDW method had a higher prediction efficiency than other methods including kriging and cokriging methods.

In this paper, both interpolation methods ordinary kriging using GS+ software version 10 and Inverse Distance Weighted method (IDW) in ArcView GIS 'spatial analyst' module were used to estimate the soil salinity spatial distribution in the irrigated perimeter of 'Zelba 1' of the region of Mahdia (Eastern Tunisia). The choice of methods was based on accuracy and suitability in analyzing and predicting the spatial distribution of soil salinity. In fact, the electrical conductivity ($EC_{1/5}$) measurements obtained from the five soil layers within the irrigated perimeter, as reported by (Louati *et al*., 2018) were subsequently interpolated in this study. They were geo-statistically analyzed by GS+ software version 10 program and then interpolated by ordinary kriging. The same ($EC_{1/5}$) data were also analyzed using IDW tool in the ArcView GIS 3.2 'spatial analyst' extension. The performances of interpolation were evaluated and compared. Then, the obtained maps from both methods were interpreted and discussed.

2. Methodology

2.1 Study area

The irrigated perimeter Zelba is located in the Zelba area, covering 2800000 m^2, south of Sidi Alouane in the region of Mahdia of eastern Tunisia (**Figure1a** and **Figure 1b**). The research area covers approximately 600000 m^2, divided into twenty plots of 30000 m^2 each (**Figure 1c**), all supplied with saline water pumped from a well topping into a deep aquifer of the Sahel of Sfax 1. This area is coordinated between 35◦14’08.76’’ North.10◦51’39.51’’ East. It has a geomorphological plane with a low-angle slopes of less than 3% grade, indicating a relatively flat land. In addition, the study area experiences a semi-arid and arid climate. The average temperature is 19°C and the mean annual precipitation is 289 mm. The soil type is deep isohumic according to the World Reference Base for Soil Resources (Fu *et al*., 2021). This soil presents a silty texture at the surface to silty-clay texture in the deep layers (Ben hassine *et al*., 1988). The soil sampling points and the electrical conductivity ($EC_{1/5}$) measurements locations are shown in **Figure 1c**, as reported by (Louati *et al*., 2018). The total dissolved (solids) TDS in the water well of the perimeter is estimated at 5000 mg/l (Hachicha, 1994). According to (Lentz, 2021), irrigation water with TDS greater than 5000 mg/l may interact with accumulated salts in soils and negatively influence soils and even groundwater quality and crop productivity.

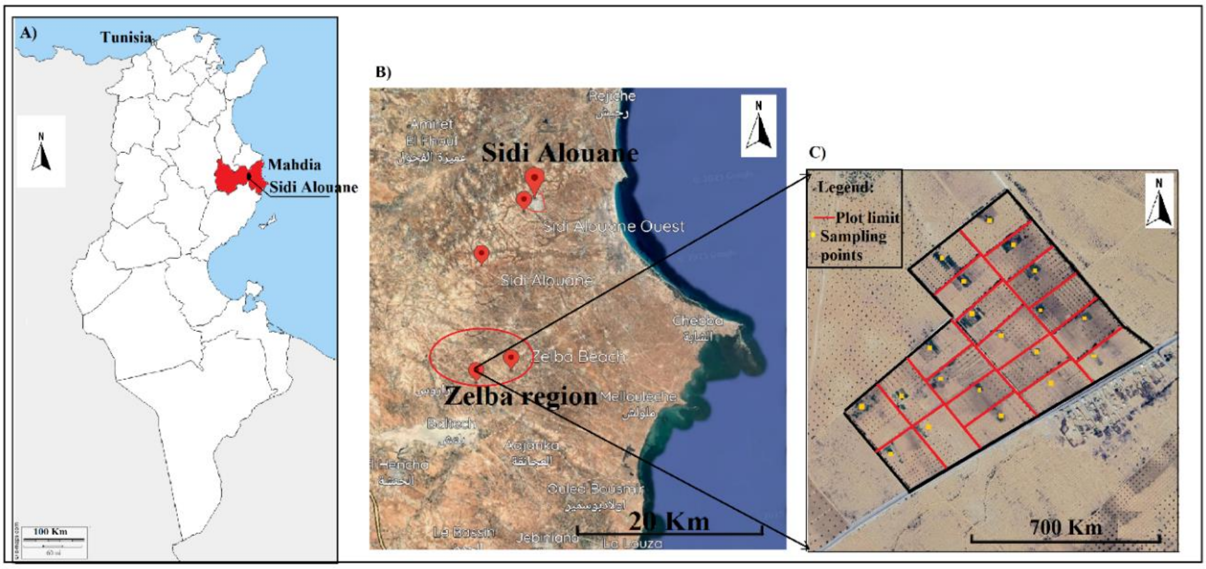

Figure 1. Locations of the study area and sampling points

2.2 *Geostatistical analysis and interpolation methods*

2.2.1 Ordinary kriging interpolation using GS+ software

A high-resolution satellite image was extracted from Google Earth. The coordinates of each sampling point of the soil (X, Y and Z) were then, identified. The obtained coordinates and $EC_{1/5}$ data measured in five soil layers of the irrigated perimeter were geo-statistically analyzed using GS+ software version 10 program. Calculated semi-variograms were obtained and maps of $EC_{1/5}$ were interpolated by ordinary kriging (OK).

Semi-variogram

The prime mechanism in geostatistics is the semi-variogram, which defines the local dependence between neighboring datasets. Semi-variograms were used to identify soil sampling locations (Webster and Oliver, 2001). They are a key tool in the theory of regionalized variables and are formed by three basic parameters: nugget, which is the unexplained variability at zero distance. The range, which is the distance beyond which there is no spatial correlation and the sill that represents the variability of spatially independent samples (Karnieli and Gilead, 2009). Together, these parameters describe the spatial structure as the following **Eqn.1** (Muhammad Saleh, 2018):

$$\gamma\ (h) = C_0 + C \qquad \textbf{Eqn.1}$$

γ (h) : semi-variance for the distance interval class h, C_0 : Nugget effect, C: Structured variance.

In this study, semi-variograms were calculated for $EC_{1/5}$ measured in five layers in the irrigated perimeter. These semi-variograms were adjusted by a Gaussian model based on the highest coefficient of determination r^2 and the lowest variance in order to improve the spatial analysis of the salinity in the irrigated perimeter.

Cross validation

Cross validation is a suitable tool for testing interpolation methods (Dubrule, 1981) cited by (Dellino *et al*., 2012). It involves omitting one data point at a time and determining how well this point can be estimated from the other data. According to INERIS report, cross validation is a statistical method. It is used to select the best variogram model and the most appropriate kriging type by comparing estimated and true values to find the model with highest correlation (LCSQA, 2003). In this study, cross validation was calculated to validate the semi-variogram model and evaluate the performance of ordinary kriging. The analyzed parameters are Regression coefficient (R) and correlation coefficient (r^2) between measured and estimated values. r^2 was applied to determine goodness of fit (Robertson, 2008).

Ordinary kriging (OK)

Ordinary kriging (OK) is a commonly used method in spatial interpolation for environmental data (Emery, 2005), (Afzal *et al*., 2011), (Li *et al*., 2022). This method gives the local correlations between scores to estimate a mean level at a non-sampled site (Kasmaee *et al.*, 2010). Some studies, such as (Rakotonirina *et al*., 2024), (Raghuvanshi and Tiwari, 2023) have used ordinary kriging to perform spatial interpolation of soil salinity. These studies have received higher ratings. (Matheron, 1967), (Abed *et al*., 2014) suggest that the ordinary kriging methods produced more homogeneous results than the other interpolation methods in predicting and mapping saline soil and proved to be the best estimator. In this study, soil salinity spatial prediction maps were produced by the ordinary kriging procedure obtained by GS+ software version 10, using semi-variograms. Besides, the ordinary kriging was used for data generation from small scale mapping.

2.2.2 Inverse Distance Weighted (IDW) in ArcView GIS 'Spatial analyst' module

ArcView GIS 'Spatial analyst' module was used by many researchers for various purposes. For instance, (Lemenkova, 2015) used this application to predict and map chemical pollution of the water.

ArcView GIS 'Spatial analyst' module was also used by (Dakhinat, 2007) to predict the spatial variation of irrigated soil properties of the region of Biskra (Algeria). In this study, the satellite image extracted from Google Earth was georeferenced using (Georeferencing and transformation tool). In this image, soil sampling points were located and the $EC_{1/5}$ measurements were introduced. Then, thematic maps of $EC_{1/5}$ were created using Inverse Distance Weighted method (IDW) in ArcView GIS 'spatial analyst' extension.

Inverse Distance Weighted method (IDW)

IDW is a spatial estimation method (Liu *et al.*, 2014). It estimates the value at an unmeasured locations as a weighted average of a nearby sampling values. The weight assigned to each sample is proportional to the inverse of the distance. The IDW method is expressed by the following **Eqn** :

$$Z^{*}(x) = \sum_{i=1}^{n} wi\, \mathbf{Z}(xi) \qquad \textbf{Eqn.2}$$

$Z^*(x)$ is the estimated value at unknown location; $Z(x_i)$ represents the known value; n is the number of observations near the interpolated points; w_i is the weight assigned to each known point.

3. Results and discussion

3.1 Geostatistical analysis of the soil $EC_{1/5}$

Table 1 shows the electrical conductivity ($EC_{1/5}$) measurements obtained from the five soil layers within the irrigated perimeter, as reported by (Louati *et al.*, 2018). The obtained results were then interpolated in this study.

Table 1. Mean values of soil $EC_{1/5}$ (Louati *et al.*, 2018)

Layer (cm)	Soil $EC_{1/5}$ (S/m)			
	Min	**Max**	**Mean**	**Standard deviation**
0-30	0.07	0.13	0.097	0.018
30-60	0.08	0.15	0.116	0.023
60-90	0.09	0.16	0.132	0.020
90-120	0.13	0.165	0.147	0.012
120-150	0.135	0.18	0.157	0.009

S/m : Siemens per meter

Variography model parameters are presented in **Table 2**. In fact, the considered soil salinity exhibits a clear nugget effect in five layers of the irrigated perimeter. Values are relatively low ($C_0 \leq 10^{-4}$) implying low errors in measurements, because of small distance between sampling points. This also could be due to the land geomorphology of the studied area, characterized by mild slopes of less than 3%. The nugget effect/sill ratio calculated for five layers of the irrigated soil is less than 25% and the correlation coefficient (r^2) is close to 1 (**Table 2**). These results indicate that the spatial variation in soil properties is strongly structured and the spatial autocorrelation of $EC_{1/5}$ between sampled values is strongly positive. (Hamzaoui and Baghdadin 2021) used the nugget/sill ratio value as the criterion of spatial dependences and also demonstrated that the nugget/sill ratio value less than 25% was regarded as highly spatially dependent. The range values of different soil layers ranged between 607 and 1520 m throughout the perimeter (**Table 2**). These values are low compared to those obtained by (Samper-Calvete and Carrera-Ramirez, 1996), who showed that a great range value demonstrated that the soil property values are influenced by other values of these properties over longer distances than soil properties with lower ranges. The very high values of range could be also affected by natural and anthropogenic factors over great distances (Lopez-Granados *et al.*, 2002).

Table 2. Variography model parameters and cross validation model for soil $EC_{1/5}$

Layer (cm)	Variography model parameters						Cross validation parameters	
	C_0 (m^2)	P (m^2)	C_0/P (%)	A (m)	$C/(C_0+C)$	r^2	R	r^2
0-30	$2.3\ 10^{-3}$	$4.2\ 10^{-2}$	0.054	915	0.945	0.855	0.99	0.805
30-60	$5.9\ 10^{-3}$	$8.2\ 10^{-2}$	0.0720	1130	0.929	0.925	0.97	0.785
60-90	10^{-4}	0.157	$6.36\ 10^{-4}$	1520	0.999	0.970	0.94	0.865
90-120	10^{-3}	0.022	0.045	950	0.952	0.785	0.92	0.722
120-150	10^{-3}	$8\ 10^{-3}$	0.125	607	0.87	0.722	0.850	0.650

C_0 : Nugget effect ; P : C_0+ C, Sill ; C_0/P : Nugget effect/ Sill ; A : range ; r^2 : Correlation coefficient ; R : Regression coefficient

Thus, the findings reveal that the modeled Gaussian semi-variograms highlight a well-defined spatial structure of soil salinity across the irrigated perimeter. These results are similar to those found by (Zhao *et al.*, 2016). These authors used a sequential Gaussian simulation to assess the uncertainly of the spatial distribution of soil salinity in arid regions of Northwest China by applying the experimental semi-variograms obtained by GS+ 9.0 software package. These semi-variograms showed the existence of a good spatial structure in soil salinity. (Bhunia *et al.*, 2018) demonstrated that spherical, exponential and stable semi-variogram model was found to be best fit for groundwater quality, where the nugget effect values were very low.

Cross validation was adopted to validate the semi-variogram model and to evaluate the performance of ordinary kriging interpolation method. Results showed that the correlation coefficient (r^2) values are close to 1 and the regression coefficient values (R) ranged between 0.85 and 0.99 in the irrigated soil, suggesting low cross validation errors (**Table 2**). Hence, cross validation indicates that the semi-variogram model is a good and satisfactorily fit. Many investigators also employed cross validation method to choose the best model for interpretation, using the kriging model (Behera and Shukla, 2015, Behera *et al.*, 2016).

3.2 Spatial distribution of the soil salinity using two interpolation methods

The general trends of the spatial distributions of the soil salinity obtained using the two interpolation methods were similar. Spatial interpolation maps established by the ordinary kriging (**Figure 2a**) and Inverse Distance Weighted method (IDW) (**Figure 2b**) showed a slight spatial variation in $EC_{1/5}$ in five soil layers of the irrigated perimeter. Repartition of maps showed also that this salinity increased slightly with depth.

Indeed, the $EC_{1/5}$ values in the deep soil layer (120-150 cm) were found to be higher than at the 0-30 cm soil layer. Mean $EC_{1/5}$ values ranged between 0.007 and 0.13 S/m at the surface (0-30 cm) indicating a moderate saline soil and between 0.13 and 0.18 S/m in the deep layer (120-150 cm) indicating a saline soil based on the United States Salinity Laboratory; (USSL, 1954) classification. In fact, the increase in the soil salinity with depth is explained by the fact that the upper layer is characterized by silty texture. Thus, it has undergone an infiltration of salts from irrigation water. Deeper down, characterized by fine textured soil, the slow movement of salts explains the increasing trend of $EC_{1/5}$. Thus, the soil texture has an influence on the soil salinity and it may control the soil salinity distribution in this perimeter.

Obtained maps also showed that the higher values of $EC_{1/5}$ were detected in the southern and southwestern parts of the perimeter, especially in the deep layer (**Figure 2a** and **Figure 2b**). The low salinity recorded in the northern section of the area may be linked to its closeness to the water well. This area likely receives a greater water supply, partly due to overflow from the nearby basins, which enhances the salts leaching into deeper layers.

Figure 3 showed a low standard deviation in maps, where values varied between 0.001 and 0.032. This, demonstrates reliable interpolation and thus a high mapping accuracy. This study revealed that obtaining detailed soil maps is important to provide a valuable reference for the prediction of soil salinity, develop targeted strategies and identify problematic regions.

Although interpolation methods may have similar accuracies, many researchers argue that ordinary kriging is more precise than other methods because it uses variograms model, cross validation techniques and uncertainty measures to examine spatial correlation. For instance, (Emadi and Baghernejad, 2014) demonstrated that the ordinary kriging method had the minimum error compared with conditional simulations methods in the agricultural coastal areas of northern Iran. As reported by (Eldeiry and Garcia, 2010) the performance of the different geostatistical models, in the southern part of Arkanas River Basin in Colorado, USA, were as follows: ordinary kriging> regression kriging> cokriging. In the work of (Fu *et al.*,2021) different interpolation methods were found to be optimal for the different soil characteristics and layers. (Hamzaoui and Baghdadi, 2021) used ordinary kriging techniques to estimate the spatial variability of soil characteristics in Beni Moussa irrigated perimeter (Talba plain Morocco). The obtained maps were very useful in the selection of appropriate interventions, in particular of conservation and rehabilitation of deteriorated soils. Meanwhile, in some studies, ordinary kriging and Inverse Distance Weighted (IDW) have been rated equally (Antal *et al.*, 2021).

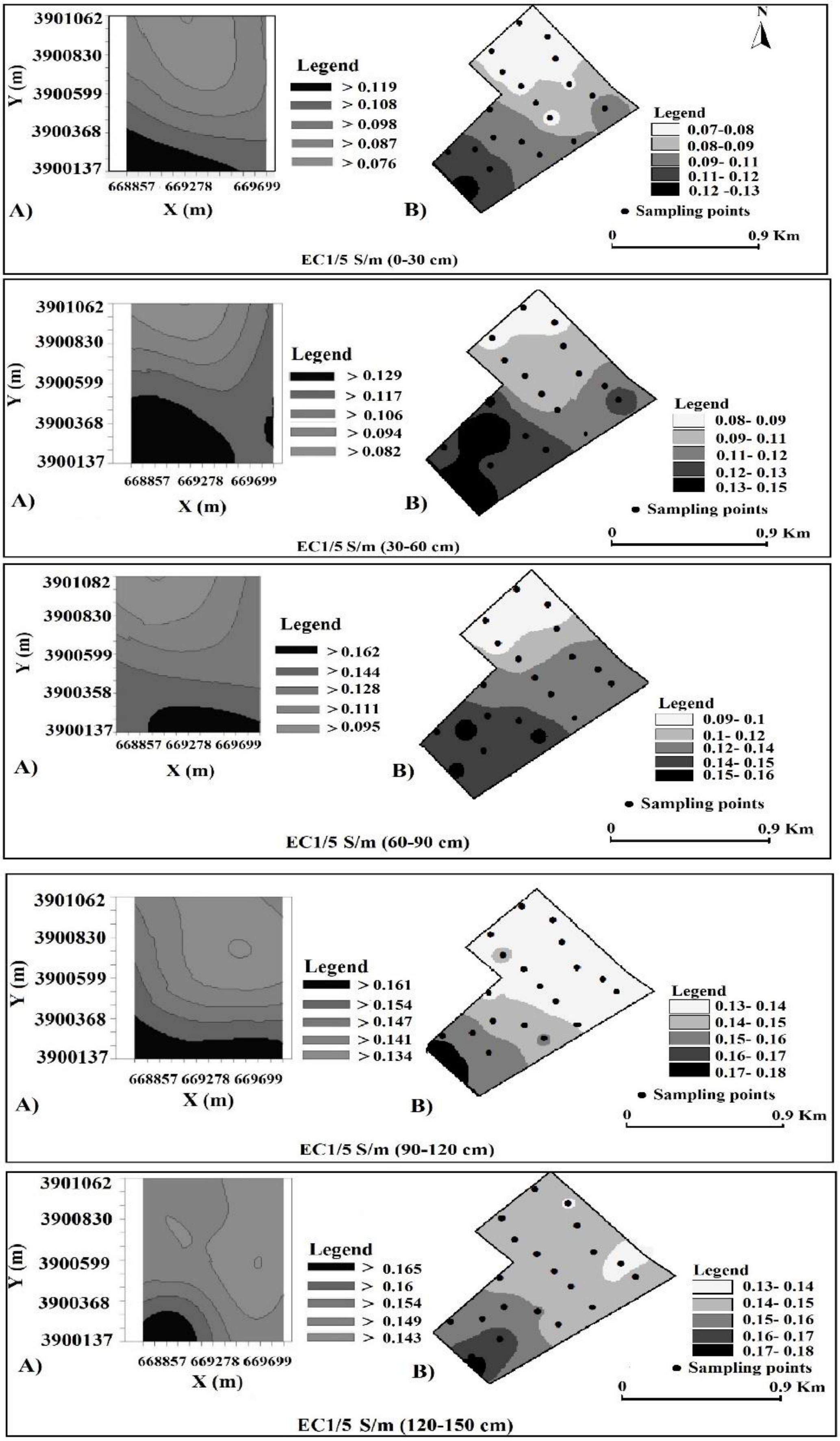

Figure 2a. Spatial distribution of $EC_{1/5}$ using ordinary kriging; **b)** Spatial distribution of $EC_{1/5}$ using ArcView GIS'spatial analyst' module

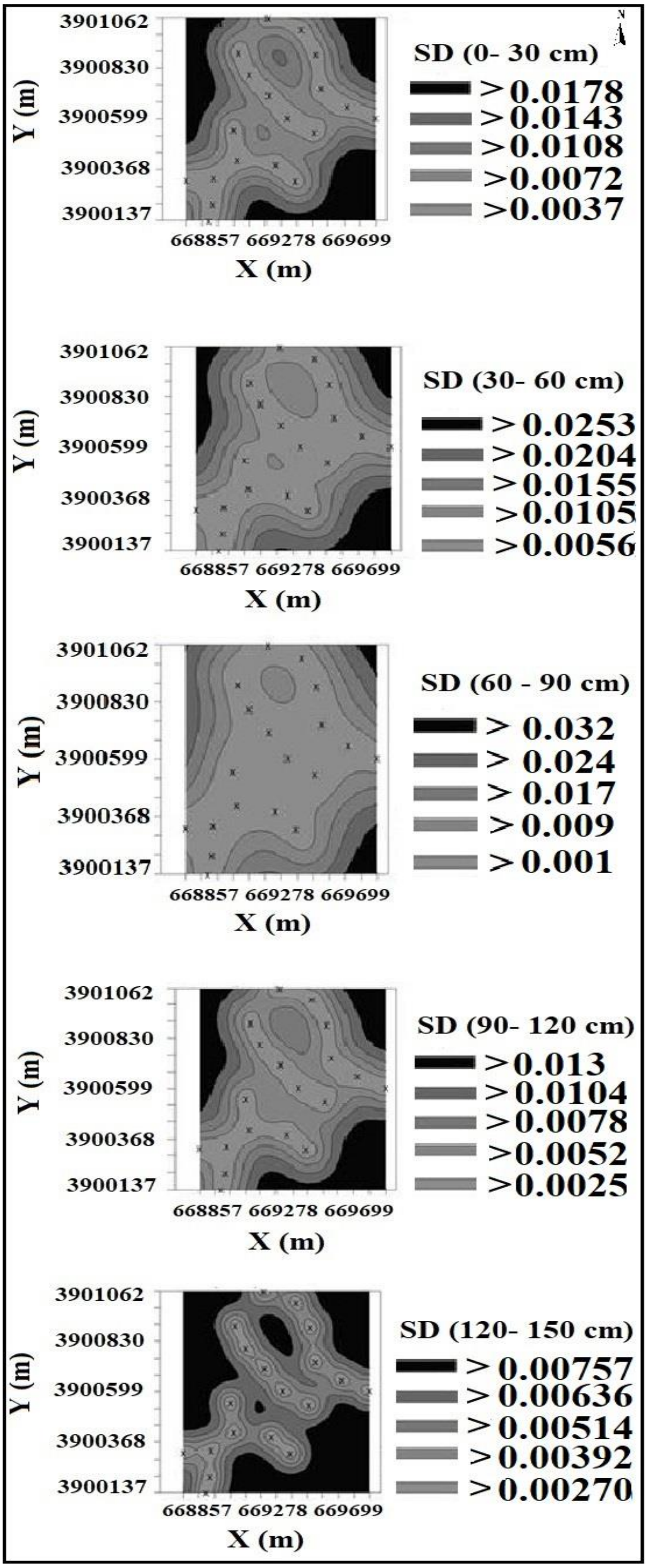

Figure 3. Standard deviation (SD) maps of soil salinity spatial distribution

Conclusion

Accurately mapping the spatial distribution pattern of soil salinity is crucial for sustainable soil management and decision making. Ordinary kriging using GS+ software version 10 and Inverse Distance Weighted method (IDW) in ArcView GIS 'spatial analyst' module were applied to predict the spatial distribution of soil salinity in the irrigated perimeter Zelba of the region of Mahdia (Eastern Tunisia). Spatial maps of soil salinity generated by two interpolation methods showed similar distribution pattern. Furthermore, an increase in the soil salinity with depth was observed. This increase is primarily caused by the soil texture. Indeed, the upper soil layer is characterized by silty texture. Thus, it has undergone an infiltration of salts from irrigation water. In deep layers, characterized by fine textured soil, the slow movement of salts explains the increasing trend of $EC_{1/5}$. Spatial maps revealed a slight spatial variation in $EC_{1/5}$ in five layers of the irrigated perimeter. The highest values of $EC_{1/5}$ occurred in the southern and the southwestern parts of the studied area. In fact, these parts receive less water than the northern part which is much closer to the drilling water well. This latter exhibited low soil salinity because it receives more water by the overflow from the existing basins facilitating the salts leaching in depth. These findings highlight the importance of the soil quality assessment for managing soil health, and elaborating sustainable irrigation managements and environmental decision. The results obtained may be improved by integrating more advanced methodologies, such as Machine Learning.

Acknowledgment, Authors thank the High Institute of Agronomy of Chott Mariem of Sousse, Tunisia for help with measurements at the laboratory and in the field. This study was supported by the Research Unit of the Applied Hydrosciences of the Institute of Sciences and Technology of Water (Gabes, Southern Tunisia).

Disclosure statement: *Conflict of interest*: The authors declare that there are no conflicts of interest.
Compiliance with Ethical Standards: This article does not contain any studies involving human or animal subjects.

References

Abed A. M., Saffarini G.A., Sadaqah R.M. (2014) Spatial distribution of uranium and vanadium in the upper phosphorite member in Eshidiyya basin, southern Jordan, *Arab. J. Geosci*., 7, 253–271. 10.1007/s12517-013-0837-1

AbdelRahman M.A.E., Zakarya Y.M., Metwaly M.M., Koubouris G. (2021) Deciphering Soil Spatial Variability through Geostatistics and Interpolation Techniques, *Sustainability.*, 13, 194. https://doi.org/10.3390/su13010194

Abdennour M.A., Douaoui A., Bradaï A., Bennacer A., Fernández M.P. (2019) Application of kriging techniques for assessing the salinity of irrigated soils: the case of El Ghrous perimeter, Biskra, Algeria. Span. *J. Soil Sci*, 9(2)., 105-124. 10.3232/SJSS.2019.V9.N2.04

Afzal P., Alghalandis Y.F., Khakzad A., Moarefvand P., Omran N.R. (2011) Delineation of mineralization zones in porphyry Cu deposits by fractal Concentration–Volume modeling, *J. Geochem. Explor*., 108, 220–232. http://dx.doi.org/10.1016/j.gexplo.2011.03.005

Antal A., Guerreiro P.M.P., Cheval S. (2021) Comparison of spatial interpolation methods for estimating the precipitation distribution in Portugal, *Theor. Appl. Climatol*., 145 (2), 1193–1206. 0.21203/rs.3.rs-329689/v1

Awedat M.A., Zhu Y., Bennet J.M., Raine S.R. (2021) The impact of clay dispersion and migration on soil hydraulic conductivity and pore networks, *Geoderma.*, 404, 115297. 10.1016/j.geoderma.2021.115297

Bartels D., Sunkar R. (2005) Drought and Salt Tolerance in Plants, *Crit. Rev. Plant Sci.*, 24, 23–58. 10.1080/07352680590910410

Behera S. K., Shukla A. K. (2015) Spatial distribution of surface soil acidity, electrical conductivity, soil organic carbon content and exchangeable potassium, calcium and magnesium in some cropped acid soils of INDIA, *Land Degrad. Dev.*, 26 (1), 71-79. https://doi.org/10.1002/ldr.2306

Behera S. K., Suresh K., Rao B. N., Mathur R. K., Shukla A. K.; Manorama K. (2016) Spatial variability of some soil properties varies in oil palm (Elaeis guineensis Jacq) plantations of west coastal area of India, *Solid Earth.*, 19, 10–24. https://doi.org/10.5194/se-7-979-2016

Ben Hassine H., Hachicha M., Job J.O. and Loyer J.Y. (1988), *Application of Electromagnetic conductivity to monitor soil salinity in irrigated areas of Tunisia*, *ORSTOM*, Tunisian Soil Directorate.

BhuniaG.S., Keshavarsi A., Shit K.P., Omran E.E., Bagherzadeh A. (2018) Evaluation of groundwater quality and its suitability for drinking and irrigationusing GIS and geostatistic techniques in semiraid regions of Neyshabur, Iran, *App. Water Sci.*, 8, 168. https://doi.org/10.1007/s13201-018-0795-6

Caglar A., Dengiz O. (2025) Analyzing soil erosion dynamics driven by long term land use changes: Intrgrating sustainable land use strategies, *Eurasian. J. Soil Sci.*, 14 (4), 298- 312. 10.18393/ejss.1713215

Chetouani M., Chetouani R., Loukili E., Hammouti B. (2023). The qualitative and quantitative study of Rosmarinus officinalis essential oils under the effect of water stress at the juvenile and adult stages in greenhouse, *J. Mater. Environ. Sci.*, 14(8), 967-977

Dakhinat S. (2007), SIG contribution to the spatial representation of the salinity of irrigated soil in arid environments (relationship between EC and fine fraction), Ain Benoui, Biskra, Algeria: *ESRI Francophone Conference*, Versailles, France, 27.

Dellino G., Kleijnen J.P.C., Meloni C. (2012) Rubust optimization in simlationTaguchi and Krige combined, *Informs.J. Comput.*, 24 (3), 471- 484. 10.1287/ijoc.1110.0465

Dubrule O. (1981), Kriging and splines in automatic mapping- application to petroleum examples: Thesis, ENSMP, Geostatistics Center, 35 street St. Honore, Fontainebleau, France, 150.

Eldeiry A.A., Garcia L.A. (2020) Comparison of Ordinary Kriging, Regression Kriging, and Cokriging Techniques to Estimate Soil Salinity Using LANDSAT Images, *J. Irrig. Drain. Eng. ASCE.*, 136, 355–364. 10.1061/(ASCE)IR.1943-4774.0000208

Emadi M., Baghernejad M. (2014) Comparison of spatial interpolation techniques for mapping soil pH and salinity in agricultural coastal areas, northern Iran, *Arch. Agron. Soil Sci.*, 60, 1315–1327. 10.1080/03650340.2014.880837

Emery X. (2005) Simple and ordinary multigaussian kriging for estimating recoverable reserves. *Math. Geol.*, 37, 295–319. 10.1007/s11004-005-1560-6

Fu T., Gao H., Liu J. (2021) Comparison of different interpolation methods for prediction of soil salinity in arid irrigation regions in Northern China, *Agron. J.*, 11, 1535. https://doi.org/10.3390/Agronomy:11081535

Gama J.T. (2023) The role of soils in sustainability, climate change, and ecosystem services: Challenges and opportunities, *Ecologies.*, 4, 552- 567. https://doi.org/10.3390/ecologies4030036

Gribb W.J., Robinson S.F., Hamerlinck J.D. (2005), *Applying ArcVien spatial analyst software's model builder to habitat conservation planning.* University of Wyoming, 18.

Hachicha M.,Job J.O., Mtimet A. (1994). Saline soils and salinization in Tunisia. Tunisia soils, *Bulletin of the Soil Directorate.*, 15, 270-341.

Haj Amor Z., Araya T., Kim D.G., Bouri S., Lee J., Ghiloufi W., Yang Y., Kang H., Jharia M.K., Banerjee A., Lal R. (2022) Soil salinity and its associated effects on soil microorganisms, greenhouse gaz emissions, crop yield, biodiversity and disertification: A review, *Sci. Total., Environ.*, 843, 156964. https://doi.org/10.1016/j.scitotenv.2022.156946.

Hamzaoui E.L., El Baghdadi M. (2021) Characterizing spatial variability of some soil properties in Beni-Moussa irrigated perimeter from Tadla plain (Morocco) using geostatistics and kriging techniques, *J. Sediment. Environ.*, 6, 381-394. 10.1007/s43217-021-00050-x

Hassani A., Azapagic A., Shokri N. (2021) Global predictions of primary soil salinization under changing climate in the 21st century Nat, *Commun.*, 12, 6663. 10.1038/s41467-021-26907-3.

Hu Z., Miao Q., Shi H., Freng W., Hou C., Yu C., Mu Y. (2023) Spatial variations and distribution pattern of soil salinity at Canal Scale in the Hetao Irrigation District, *Water.*, 15, 3342. https://doi.org/10.3390/w15193342

Jamil A., Riaz S., Ashraf M., Foolad M.R. (2011) Gene expression profiling of plants under salt stress, *Crit. Rev. Plant Sci.*, 30, 435–458. 10.1080/07352689.2011.605739

Karnieli A., Gilead U. (2009). Satellite image processing and geo-statistical methods for assessing land degradation around watering points in the UST- URT plateau Kazakhstan. Recent Advances in Remote Sensing and Geoinformation Processing for Land. Degradation Assesment- Roder and Hil (Ed.), *ISBN 978- 0- 415- 39769-8*. London, 313- 322.

Kasmaee S., Gholamnejad J., Yarahmadi A., Mojtahedzadeh H. (2020) Reserve Estimation of the high phosphorous stockpile at the Choghart iron mine of Iran using geostatistical modelling, *Min. Sci. Tech.*, 20, 855-860. 10.1016/S1674-5264(09)60295-7

Laita M., Sabbahi R., Elbouzidi A., Hammouti B., Messaoudi Z., Benkirane R., Aithaddou H. (2024a) Effects of Sustained Deficit Irrigation on Vegetative Growth and Yield of Plum Trees Under the Semi-Arid Conditions: Experiments and Review with Bibliometric Analysis, *ASEAN Journal of Science and Engineering*, 4(2), 167-190

Laita M., Hammouti B., Sabbahi R., Messaoudi Z., Benkirane R. (2024b) Effect of Water Regime and Soil Maintenance Mode on Vegetative Growth and Peach Tree Production, Indonesian Journal of Science & Technology, 9(1), 33-44

LCSQA. (2003), Air Quality Monitoring Central Laboratory. Study report, INERIS.

Lemenkova P. (2015) Standarization of the thematic mapping for environmental monitoring of the Arctic Sea. Complex Problem of Technospheric Security: *Conference*, Voronezh, Russia.

Lentz R.D. (2021) Does turbulent-flow conditioning of irrigation water influence soil chemical processes: I. Laboratory results, *Commun soil Sci Plant Anal.*, 53, 651-663. 10.1080/00103624.2021.2017964

Li Z., Tao H., Zhao D., Li H. (2022) Three-dimensional empirical bayesian kriging for soil pahs interpolation considering the vertical soil lithology, *Catena.*, 212. 106098. 10.1016/j.catena.2022.106098

Liu R., Chen Y., Sun C., Zhang P., Wang J., Yu W., Shen Z. (2014) Uncertainty analysis of total phophorus spatial-temporal variations in the Yangtze River Estuary using different interpolation methods, *Mar. Pollut. Bull.*, 86. 10.1016/j.marpolbul.2014.07.041

Lopez-Granados F., Jurado-Exposito M., Atenciano S., Garcia-Ferrer A., De la Orden M. S., Garcia-Torres L. (2002) Spatial variability of agricultural soil parameters in southern Spain, *Plant and Soil.*, 246, 97-105. 10.1023/A:1021568415380

Louati D., Majdoub R., Rigane H., Abida H. (2018) Effects of irrigating with saline water on soil salinization (Eastern Tunisia), *Arab.J. Sci.Eng.*, 2193- 567X. 10.1007/S13369-018-3215-1

Matheron G. (1967), *Kriging or polynomial interpolation procedures*, CIMM Trans., 70, 240–244.

Muhammad Saleh A. (2018) Spatial variability mapping of some soil poperties in Jadwal Al-Amir Project/ Babylon/Iraq, *J. Indian. Soc. Remote. Sens.*, 46, 1481- 1495. https://doi.org/10.1007/s12524-018-0795-x

Panday D., Maharjan B., Chalise D., Shrestha R.K., Twanabasu B. (2018) Digital soil mapping in the Bara district of Nepal using kriging tool in ArcGIS, *PloS one.*, 13(10), e0206350. 10.1371/journal.pone.0206350.

Pouryazdankhah H., Shahnazari A., Ahmadi M.Z., Khaledian M., Andersen M.N. (2019) Rice yield estimation based on forecasting the future condition of groundwater salinity in the Caspian coastal strip of Guilan Province, Iran. *Environ. Monit. Assess.*, 191, 492. 10.1007/s10661-019-7613-y

Raghuvanshi A. S., Tiwari H. L. (2023) Comparison of spatial interpolation methods for mapping seasonal groundwater levels. Geospatial and Soft Computing Techniques, *Proceedings of 26th International*

Conference on Hydraulics, Water Resources and Coastal Engineering., Singapore. 10.1007/978-981-99-1901-7_19.

Rakotonirina H., Honeine P., Atteia O., Van Exem A. A. (2024) generative deep neural network as an alternative to co-kriging, *App Comput Geosci.*, 24, 100198. https://doi.org/10.1016/j.acags.2024.100198.

Robertson G.P. (2008*), GS+: Geostatistics for the environmental sciences. Gamma Design Software version 10.* Plainwell, Michigan 49080, USA, ISBN number 0-9707410-0-6.

Sahbeni G., Székely B. (2021) Spatial modeling of soil salinity using kriging interpolation techniques: A study case in the Great Hungarian Plain. Eurasian, *J. Soil Sci*., 11 (2), 102- 112. 10.18393/ejss.1013432

Samper-Calvete F. J., Carrera-Ramírez J. (1996), Geostadística aplicaciones a la hidrología subterránea centro internacional de métodos numéricos en ingeniería. España: Universitat Politècnica de Catalunya, 484.

Setia R., Gottschalk P., Smith P., Marschner P., Baldock J., Setia D., Smith J. (2013) Soil salinity decreases global soil organic carbon stocks, *Sci. Total Environ.*, 465, 267-272. 10.1016/j.scitotenv.2012.08.028

Shrivastava P., Kumar R. (2015) Soil salinity: A serious environmental issue and plant growth promoting bacteria as one of the tools for its alleviation, *Saudi J. Biol. Sci.*, 22, 123–131. https://doi.org/10.1016/j.sjbs.2014.12.001

Tomaszewski B. (2021). Geographic information systems (GIS) for disaster management. CRC Press.

Uri N. (2018) Cropland soil salinization and associated hydrology: trends, processes, and examples, *Water.*, 10(8), 1030. https://doi.org/10.3390/w10081030.

US Salinity Laboratory Staff (USSL). (1954). *Diagnosis and improvement of saline and alkali soils. US Department of Agriculture,* Handbook n°60, U.S. Gov. Print, Office.Washington D.C., 160.

Wang N., Chen S., Huang J. (2024) Global soil salinity estimation at 10 m using multi-source remote sensing, *Int. J. Remote Sens.*, 4 (1), 0130. 10.34133/remotesensing.0130.

Wang N., Peng J., Chen S., Huang J., Li H., Biswas A., He Y., Shi Z. (2022) Improving remote sensing of salinity on topsoil with crop residues using novel indices of optical and microwave bands, *Geoderma*., 422, 115935. 10.1016/j.geoderma.2022.115935.

Webster R., Oliver M.A. (2001), *Geostatistics for environmental scientist*. Wiley, Chichester, England.

Xu X., Huang G., Sun C., Pereira L. S., Ramos T. B., Huang Q., Hao Y. (2013) Assessing the effects of water table depth on water use, soil salinity and wheat yield: Searching for a target depth for irrigated areas in the upper Yellow River basin, *Agric. Water Manag.*, 125, 46–60. 10.1016/j.agwat.2013.04.004

Yang P., Byrne J.M., Yang M. (2016) Spatial variability of soil magnetic susceptibility, organic carbon and total nitrogen from farmland in northern China, *Catena.*, 145, 92–98. http://dx.doi.org/10.1016/j.catena.2016.05.025.

Yu J., Li Y., Han G., Zhou D., Fu Y., Guan B., Wang G., Ning K., Wu H., Wang J. (2014) The spatial distribution characteristics of soil salinity in coastal zone of the Yellow River Delta, *Environ. Earth Sci*., 72, 589–599. 10.1007/s12665-013-2980-0

Zhao Y., Feng Q., Yang H. (2016) Soil salinity distribution and its relationship with soil particle size in the lower reaches of Heihe River, Northwestern China, *Environ. Earth Sci.*, 75, 810. 10.1007/s12665-016-5603-8

(2026) ; http://www.jmaterenvironsci.com